J Mater Sci (2011) 46:7603–7610
DOI 10.1007/s10853-011-5736-9

Formation of semitransparent $CuAlSe_2$ thin films grown on transparent conducting oxide substrates by selenization

J. López-García · C. Guillén

Received: 22 March 2011 / Accepted: 21 June 2011 / Published online: 29 June 2011

Abstract Wide band-gap semiconductors have been studied for applications as buffer layers in thin film solar cells and as top cell in tandem devices. $CuAlSe_2$ (CAS) thin films were deposited onto bare and two different transparent conducting oxide (TCO)-coated glass substrates, In_2O_3:Sn (ITO) and ZnO:Al (AZO), by a two stage process consisting on the selenization of metallic precursor layers. Homogeneous and crystalline formation of CAS thin films is not trivial and it is strongly influenced by selenization conditions, type of substrate and the film thicknesses. Under certain conditions, polycrystalline $CuAlSe_2$ thin films with chalcopyrite structure and preferential orientation along the (112) plane were obtained onto bare glass susbtrates. However, formation and crystallization of homogeneous CAS thin films was promoted by transparent conducting oxides (ITO and AZO)-coated glass substrates and take place in a wide range of thicknesses and Se amounts with high degree of reproducibility. TCO-coated substrates promoted larger grains when the CAS compound was formed. The band-gap energy, preferential orientation, crystallite size and the average surface roughness varied depending on the film thickness and type of substrate.

Introduction

The ternary and quaternary Cu-based chalcopyrites are a family of semiconductors widely used in optoelectronic devices. Wide-bandgap chalcopyrites, such as $CuAlSe_2$ (CAS) with a gap energy $E_g \sim 2.67$ eV [1], have attracted great interest due to can be used as window layer or in tandem solar cells.

Although the highest efficiencies (19.9% [2]) have been achieved by alloying $CuInSe_2$ with Ga on $Cu(In,Ga)Se_2$ (CIGS)-based solar cells, Ga is expensive and scarce [3]. A more inexpensive and abundant alternative is the alloy with Al. Owing to that the optical band-gap can be varied in a wider range from $CuInSe_2$ to $CuAlSe_2$, a lesser aluminium concentration than gallium is required to achieve a similar bandgap. $Cu(In,Al)Se_2$-based solar cells with efficiencies of 16.9% have been achieved [3]. The behaviour of the quaternary compound will be affected or linked by the respective ternary, CIS and CAS. Therefore, since CIS is a well-known material [4], a deeper knowledge of the $CuAlSe_2$ films is essential to achieve high efficiency solar cells.

In order to increase the cell performance and up-scaling at low cost with high quality, several manufacturing methods and alternative solar cells configurations have been investigated and developed. An interesting manufacturing process for CAS samples, alternative to the commonly used co-evaporation [5, 6], is the two stage process consisting on the evaporation of metallic precursor layers and the subsequent annealing in a selenium environment [7–9]. This deposition method allows the individual control of the thicknesses of the metallic precursor layers which have effects on the morphological, structural and opto-electronic properties of the selenized CAS films.

Regarding to alternative solar cell configurations based on chalcopyrite compounds, multi-junction (tandem) devices have attracted lately great interest. The replacement of the commonly used opaque Mo back contact by transparent and conductive oxides (TCO) is necessary to obtain semitransparent structures. In these cases, a wide-bandgap

J. López-García (✉) · C. Guillén
Department of Energy, CIEMAT, Avda. Complutense, 22, 28040 Madrid, Spain
e-mail: juan.lopez@ciemat.es

semiconductor such as $CuAlSe_2$ and a transparent back contact are required for the upper cell. For co-evaporated CIGS and CGS-based thin films solar cells, the use of tin-doped indium oxide (ITO) and aluminium-doped zinc oxide (AZO) as transparent and conductive back contact has been reported by several authors [10–15]. However, no works have been reported with CAS onto TCO back contact.

In this study, the influence of the bare and TCO-coated substrates on the formation and properties of $CuAlSe_2$ thin films have been investigated as well as the effects of the sample thickness and the amount of Se applied in the selenization process.

Experimental details

TCO-coated substrates

Deposition of the TCO thin films was performed by magnetron sputtering from oxide ceramic targets (In_2O_3:SnO_2 90:10 wt% for ITO and ZnO:Al_2O_3 98:2 wt% for AZO) onto conventional soda lime glass (SLG). Glass substrates were placed in a vertical frame and moved in front of the respective target for ITO or AZO deposition at room temperature. After the vacuum chamber was evacuated below 2×10^{-4} Pa, high purity Ar and O_2 were introduced through independent mass flow controllers that were adjusted to obtain high transparent and conductive layers, according to previous works [16, 17]. After the deposition process, the flow of the gases was closed and the chamber was returned to a vacuum below 2×10^{-4} Pa, then annealing of the sputtered layers was carried out at 623 K during 20 min by heating with halogen lamps. In this way, ITO and AZO thin films with sheet resistance below 10 Ω/sq and visible optical transmittance above 90% were obtained [16, 17] and are used in the present study as transparent back contacts for subsequent CAS deposition.

$CuAlSe_2$ (CAS) formation

In a first stage, Cu and Al precursor layers were sequentially deposited onto bare and the TCO-coated soda lime glass substrates by e-beam evaporation of Cu and thermal evaporation of Al in a vacuum chamber with a base pressure of 10^{-5} Pa. During the precursor deposition, the substrates were rotated and an oscillatory quartz crystal microbalance monitored the growth rates and thicknesses of the individual layers. Based on previous works for the optimization of the metallic layers deposition sequence of $CuInSe_2$ [18], a SLG/(TCO)/Al/Cu/Al sequence was chosen.

In the second stage, the selenization process was performed in three steps based on the well-known temperature–time profile reported for the crystallization of $CuInSe_2$ [18] but finally increasing the temperature up to 773 K because the formation of the binary compound Al_2Se_3 starts at a temperature about 260 K higher than the formation of Cu-selenides [19]. The selenium incorporation was carried out within a partially closed graphite box with a small hole in the centre of its lid, in order to ensure an energetic over-pressure of Se during the selenization process. Enough Se will leak through the hole to balance the over pressure. Inside of this graphite box elemental Se was put together with the metallic precursor samples and loaded into a quartz tube furnace in Ar atmosphere. The Se amount was varied over a wide range for 2×6 cm^2 metallic samples areas [20].

CAS thin films of about 0.6, 1.1 and 1.7 ± 0.1 μm of thickness of only one sequence were achieved after selenization. In addition, CAS films of 1.2 ± 0.1 μm were obtained from a double sequence SLG/(TCO)/Al/Cu/Al/Al/Cu/Al and tested in order to study the effects of the thickness of the metallic precursors.

Characterization of the films

The selenized $CuAlSe_2$ thin films were characterized structural, optical and morphologically by means of X-ray diffraction (XRD) using a PHILIPS X'PERT diffractometer with CuK_α ($\lambda = 1.54056$ Å) radiation, a Perkin-Elmer LAMBDA 9 spectrophotometer at room temperature and by a JSM-6400 Scanning electron microscope (SEM), respectively. The composition of the films was determined by Energy dispersive analysis of X-rays (EDAX). The thickness and surface roughness of the selenized films were measured by means of a DEKTAK 3030 profiler.

Results and discussion

The chemical composition obtained by EDAX measurements, the thickness and arithmetic average roughness of representative CAS thin films prepared on bare and TCO-coated glass substrates are shown in Table 1. The formation of the ternary compound $CuAlSe_2$ is related with the increase on the Se (%at) incorporation. In general, TCO-coated substrates promoted the Se incorporation regarding to CAS films onto bare SLG and a higher formation and crystallization of $CuAlSe_2$ was obtained for samples deposited on TCO substrates.

Figure 1 shows XRD diagrams of Al/Cu/Al (and a double Al/Cu/Al sequence) metallic layers evaporated onto bare SLG after heating (selenization) at 773 K for different precursor thicknesses and a wide range of Selenium

Table 1 Representative data of Se supplied during the selenization Se (mg), Se incorporation Se/(Cu + Al), arithmetic average roughness $\overline{R_a}$and average crystallite size S of representative $CuAlSe_2$ thin films onto different substrates

Structure	t (μm)	Se (mg)	Se/M	R_a (nm)	S (nm)	Se (mg)	Se/M	R_a (nm)	S (nm)
SLG/CAS	0.6	120	0.03	22	–	240	0.09	56	–
SLG/CAS	1.1	120	0.12	59	–	240	0.82	187	161
SLG/CAS	1.2	120	0.12	95	–	240	1.44	83	124
SLG/ITO/CAS	0.6	120	0.84	127	189	240	1.69	184	128
SLG/ITO/CAS	1.1	120	0.86	206	183	240	0.83	142	163
SLG/ITO/CAS	1.2	120	0.90	274	172	240	0.95	253	129
SLG/ITO/CAS	1.7	120	1.27	258	137	240	0.64	300	159
SLG/AZO/CAS	0.6	120	0.95	119	175	240	1.90	146	196
SLG/AZO/CAS	1.1	120	0.86	279	167	240	0.73	202	160
SLG/AZO/CAS	1.2	120	0.70	247	185	240	0.75	178	198
SLG/AZO/CAS	1.7	120	0.83	303	214	240	0.68	120	175

amounts. For simplicity, only sample selenized with 120 and 240 mg of Se are shown. For samples with an overall thickness lesser than 1 μm or selenized with <240 mg of Se, peaks corresponding to Cu_xSe_y secondary phases (identified mainly as CuSe and Cu_2Se with JCPDS no. 49-1456 and no. 88-2043/44/45, respectively) [21–23] were detected as well as inter-metallic phases with different Cu–Al stoichiometry such as CuAl (JCPDS no. 65-1228), Cu_9Al_4 (JCPDS no. 24-0003 and 65-3347) or $Cu_{6.10}Al_{3.89}$ (denoted as Cu_xAl_y and identify with JCPDS file no. 19-0010). In addition, phases that can be related to $CuSeO_3$ (JCPDS no. 46-0790 or 70-0244) and Al_2Se_3 (JCPDS no. 19-0048) were detected.

However, the formation and crystallization of the ternary compound $CuAlSe_2$ on bare SLG is achieved increasing the overall film thickness and with the highest Se amount (240 mg of Se) independently of the metallic layer thicknesses. XRD diagrams (Fig. 1) showed peaks related to polycrystalline $CuAlSe_2$ thin films with chalcopyrite structure and preferred orientation along the (112) plane. The $CuAlSe_2$ standard file (JCPDS no. 44-1269) was used [24] to identify the reflections. The formation of the ternary compound $CuAlSe_2$ is clearly identify by the (112) reflection at ~27.72° and the doublets (220/204) at 45.77° and 46.27° (with inter-planar spacing (d) 1.98 and 1.96 Å) and (312/116) at 54.38° and 55.27°, respectively. The reflections related to Cu–Al phases are located mainly at 44.08°, 44.72° and 45.08° with inter-planar spacing (d) 2.05, 2.02 and 2.00 Å, respectively, so the peaks are unmistakably separated. The same argument for the Cu–Se phases has been detailed earlier [20, 25]. The chalcopyrite structure has been identified from the splitting of the structure lines (220)/(204) and (312)/(116) due to the tetragonal distortion (c/a ≠ 2).

Figure 2 shows clearly that the presence of TCO layers as CAS substrates promote the formation of polycrystalline

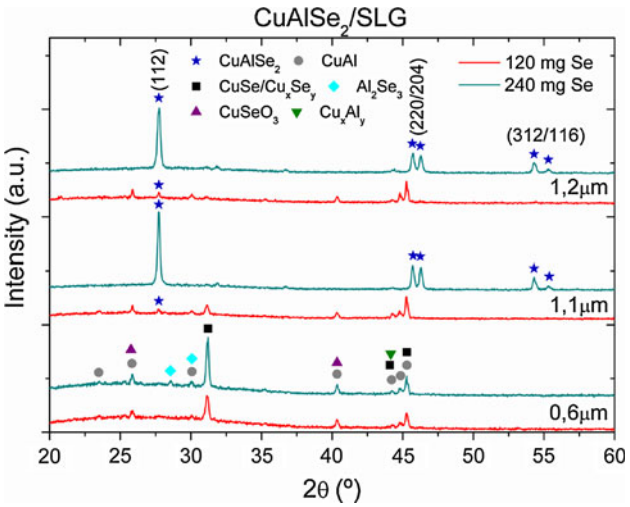

Fig. 1 XRD spectra of $CuAlSe_2$ samples with different thickness deposited onto bare substrates after heating with 120 and 240 mg of Se

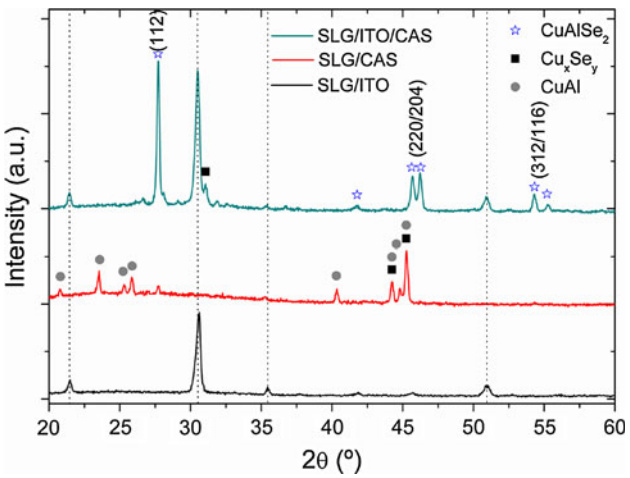

Fig. 2 XRD spectra of In_2O_3:Sn (ITO), 1.1 μm-$CuAlSe_2$ onto bare glass substrate and $CuAlSe_2$ onto ITO-coated glass substrate

$CuAlSe_2$ films. In this figure, XRD spectra of In_2O_3:Sn (ITO), 1.1 μm-$CuAlSe_2$ onto bare glass substrate and $CuAlSe_2$ onto ITO-coated glass substrate layers are displayed.

Formation of polycrystalline CAS thin films onto bare SLG strongly depends on the thickness and selenization condition. However, formation and crystallization of homogeneous CAS thin films deposited onto TCO-coated substrates take place in a wide range of thicknesses and Se amounts with high degree of reproducibility. Figures 3, 4 and 5 show the XRD diagrams of CAS samples deposited on TCO-coated substrates selenized with a wide range of Se amounts and with several thicknesses, respectively. Peaks corresponding to $CuAlSe_2$, some traces of CuSe as well as peaks related to In_2O_3:Sn (ITO) and ZnO:Al (AZO) underlayers (JCPDS no. 06-0416 and no. 05-0664, respectively) were observed. All samples deposited onto TCO-coated substrates showed a strong orientation along the (112) plane with chalcopyrite structure. Figures 3, 4 and 5 demonstrate clearly that the formation of $CuAlSe_2$ thin films is possible with a high degree of reproducibility in a wide range of thicknesses and Se amounts, contrary to the case of CAS onto bare SLG substrates.

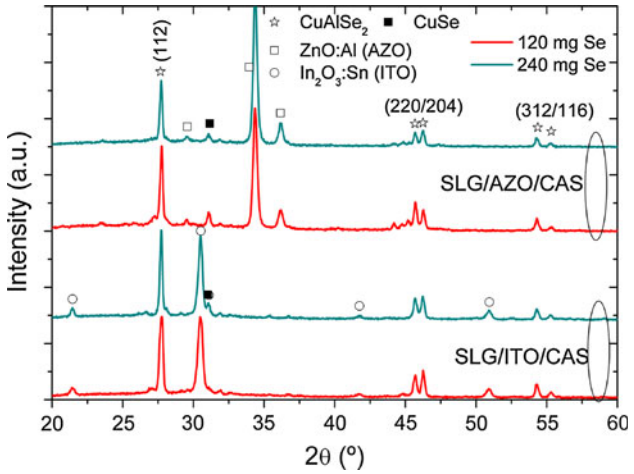

Fig. 3 Diffractograms of 1.1 μm-$CuAlSe_2$ samples deposited onto ITO and AZO-coated substrates selenized with 120 and 240 mg of Se

The average crystallite size in the (112) plane direction shown in Table 1 was estimated according to the Scherrer's formula [26]:

$$S = \frac{0.9\lambda}{B\cos\theta} \quad (1)$$

where S is the crystallite size in nm, λ the X-ray wavelength in nm, θ the diffraction angle and B the full width at half maximum (FWHM) of the diffraction peak. The average crystallite size is larger than the most of the reported data for samples deposited by this and other methods [27–29].

The preferential orientation of the crystallites along the [112] direction, F(112), was estimated by mean of the XRD patterns as the ratio between (112) peak intensity and the sum of the intensities of all peaks observed [30]. F(112) values ranging from 0.5 to 0.65 were achieved. These results are lower than the reported data for the reference material, $CuInSe_2$ [20]. However, according to the JCPDS file for $CuAlSe_2$ (F(112) ~ 0.5) the obtained orientations are higher. A slightly higher orientation along the (112) was observed for the CAS films deposited on AZO substrates at low thickness.

From optical transmission (T) and reflectance (R) data, the absorption coefficient α for the $CuAlSe_2$ films was

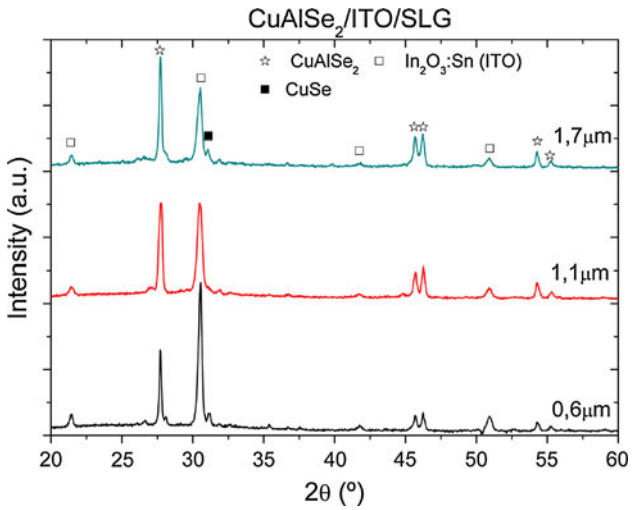

Fig. 4 XRD spectra of $CuAlSe_2$/ITO/SLG samples with different thicknesses

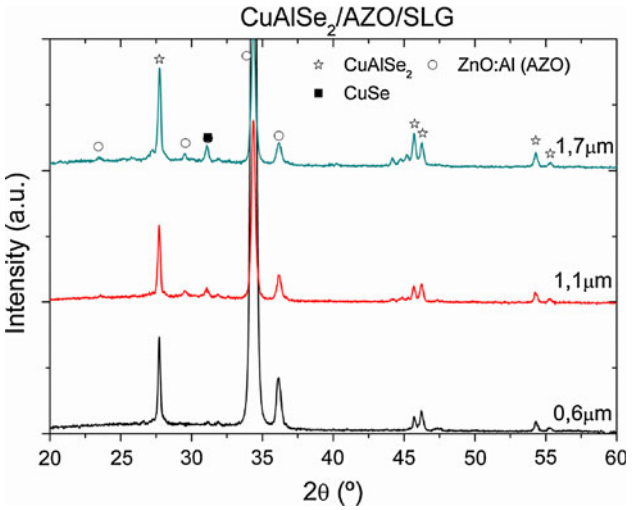

Fig. 5 XRD spectra of $CuAlSe_2$/AZO/SLG samples with different thicknesses

calculated as has been explained in an earlier work [18]. The variation of α with hν near the main absorption edge is expected to follow the relation [31]:

$$\alpha = \frac{A}{h\nu}(h\nu - E_g)^{1/2} \quad (2)$$

where A depends on the transition nature, the effective mass and the refractive index and E_g is the band-gap energy. This relation indicates that the fundamental absorption edge is due to allowed direct transitions between parabolic bands. For the $CuAlSe_2$ films, the plot of $(\alpha h\nu)^2$ versus hν from Eq. 2 determines the band-gap energy E_g by extrapolation of the linear portion of each curve as shown in Figs. 6, 7 and 8. Formation of polycrystalline CAS over bare SLG as the thickness and Se amount increase is clearly observed with the formation of an absorption edge above 2.5 eV in Fig. 6. The lack of such absorption edge and XRD peaks related to chalcopyrites in, for example, the 0.6 μm-$CuAlSe_2$/SLG sample show that remained significant Cu_xAl_y intermetallic with some Cu_xSe_y. Figures 7 and 8 illustrate that the homogeneous and crystalline formation of CAS thin films deposited on TCO-coated substrates take place in a wide range of thicknesses. The band-gap energy varied from 2.48 to 2.64 eV depending on the thickness or substrate, being lower for thinner precursor films. These E_g values are slightly lower than expected [28, 32] due to the influence of the secondary phases absorption at low energies and structural defects. Absorption below the main absorption edge can be related to band tails involving crystalline structure defects, excitonic absorption, secondary phases and other factors such as surface roughness.

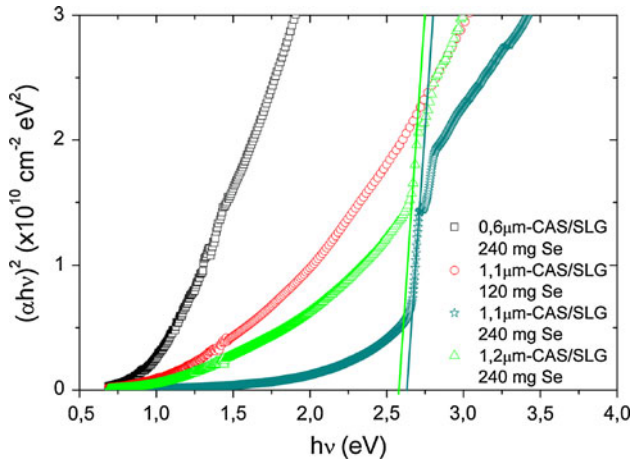

Fig. 6 Plot of $(\alpha h\nu)^2$ as a function of the photon energy for $CuAlSe_2$ samples with different thicknesses deposited on bare substrates after heating with 120 and 240 mg of Se

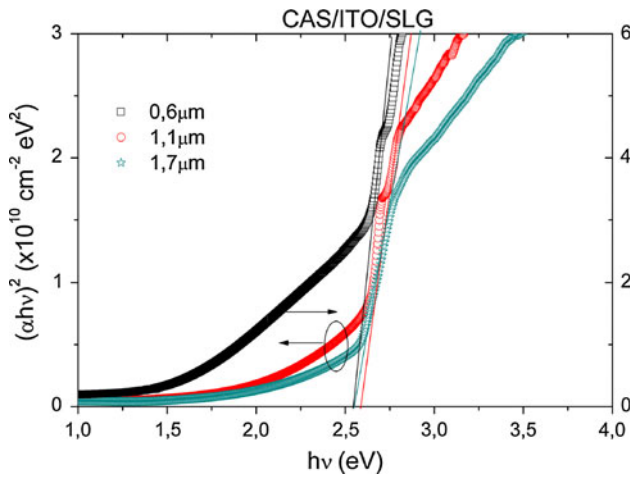

Fig. 7 Plot of $(\alpha h\nu)^2$ as a function of the photon energy for $CuAlSe_2$/ITO/SLG thin films with different thicknesses

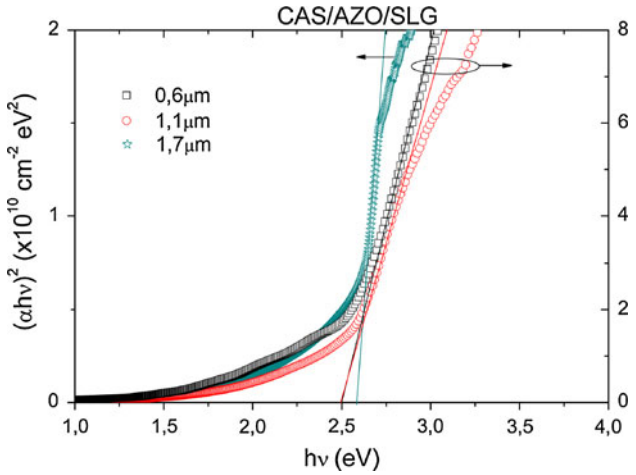

Fig. 8 Plot of $(\alpha h\nu)^2$ as a function of the photon energy for $CuAlSe_2$/AZO/SLG samples with different thicknesses

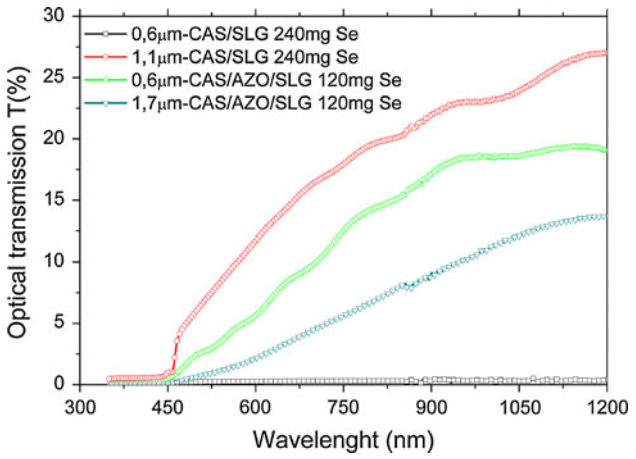

Fig. 9 Optical transmission $T(\%)$ as a function of the wavelength (nm) of CAS thin films with different substrates, thicknesses and Se amounts

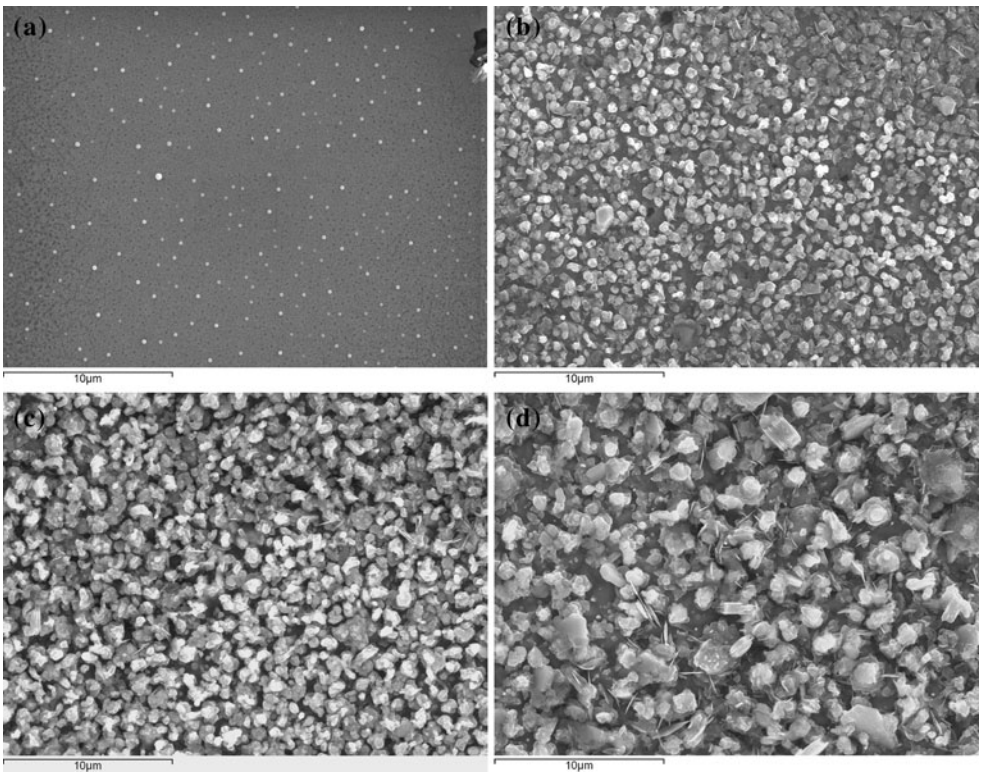

Fig. 10 SEM images of 0.6 μm-$CuAlSe_2$ thin films deposited on **a** bare SLG and **b** AZO-coated SLG substrate selenized with 120 mg of Se and 1.2 μm-$CuAlSe_2$ deposited on **c** bare SLG and **d** ITO-coated SLG

Figure 9 shows the optical transmission T(%) of several CAS samples. It is observed that the transmission enhanced as the formation and crystallization of the CAS films take place. Values around 27% at a wavelength of 1200 nm were obtained for CAS samples deposited on bare SLG substrates. Besides, transmissions above 20 and 15% have been achieved for 0.6 and 1.7 μm-CAS films deposited on transparent AZO-coated substrates, respectively. The formation of semitransparent CAS films of different thicknesses is possible over several substrates depending mainly on the thickness of the metallic precursors and Se adjustment.

The surface morphology of the CAS samples is shown in Fig. 10a–d. The formation of homogeneous and crystalline CAS samples is clearly observed in Fig. 10a, b. The thinnest layers showed an inter-metallic matrix with isolated structures related to CAS and Cu–Selenide on bare glass (Fig. 10a) whereas the formation of crystalline CAS is achieved after deposition onto AZO-coated substrate (Fig. 10b). Thicker $CuAlSe_2$ thin films deposited on bare and ITO-coated SLG are shown in Fig. 10c, d, respectively. The size of the structures observed increased with the film thickness and TCO substrates. Figure 11a, b shows the cross-sectional SEM images of ~1.7 μm-$CuAlSe_2$

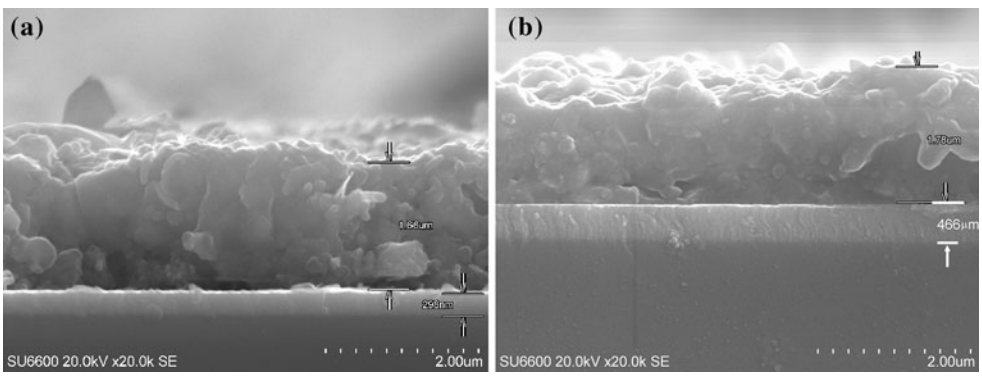

Fig. 11 Cross-sectional SEM images of ~1.7 μm-$CuAlSe_2$ thin films deposited on **a** ITO-coated and **b** AZO-coated soda lime glass substrates

samples deposited on ITO and AZO-coated substrate. Compact and crystalline layers with good adhesion to the TCO layer are observed in both pictures. However, a slight higher crystallinity on samples onto AZO is observed due to the highly crystalline substrate. Arithmetic average roughness of the CAS films surfaces shown in Table 1, measured by a profiler, enhanced when the ternary compound $CuAlSe_2$ was formed regarding to the samples with only binary intermetallic and Cu–Se phases which showed a smoother surface. It is observed a slight trend towards rougher surfaces as the thickness increase. However, it was not found a clear dependence of the roughness neither with the type of substrate nor the Se amount.

The difficulty to obtain homogeneous $CuAlSe_2$ thin films, due to the presence of active Al in the matrix, observed in Fig. 10a and XRD diagrams has been discussed in earlier works [5, 25, 33]. Based on the $CuInSe_2$ formation, the ternary chalcopyrite $CuAlSe_2$ is expected to be obtained from the reaction of Cu_2Se and Al_2Se_3. However, the formation of Al_2Se_3 starts at a temperature about 750 K [19], higher than the temperature formation of the copper selenides. Moreover, Al does not react well with Se which implies an excess of Cu–Se and Cu–Al phases as shown in Fig. 1. In addition, several studies show that the metallic or binary precursors are critical in the formation of the $CuAlSe_2$ and $Cu(In,Al)Se_2$ single phase [34, 35]. However, ITO and AZO-coated SLG substrates promoted the formation of stable chalcopyrite compounds in a wider range of experimental conditions. It has been shown that the presence of TCO-coated SLG substrates in $Cu(In,Al)Se_2$ thin films behaviour as a barrier for the oxidation from the substrate promoting a better formation [35]. Further investigations are necessary in order to a better understanding of the formation pathway of CAS and the influence of TCO substrates in its formation.

Conclusions

Formation of polycrystalline thin films of the ternary compound $CuAlSe_2$ with chalcopyrite structure onto bare SLG by selenization of the metallic precursor layers strongly depends on the thickness and selenization condition. However, formation and crystallization of homogeneous CAS thin films deposited onto transparent conducting oxides (ITO and AZO)-coated glass substrates take place in a wide range of thicknesses and Se amounts with high degree of reproducibility. In general, TCO-coated substrates promoted the Se incorporation that implies a better formation and crystallization of $CuAlSe_2$ samples. Besides, a certain overall thickness above ~ 1 μm is required to achieve the formation of the ternary compound $CuAlSe_2$ on bare SLG with the highest Se amount independently of the individual metallic layer thicknesses.

The optical transmission enhanced as the formation and crystallization of the CAS films increased. The formation of semitransparent CAS films with good adhesion to the substrate was possible over different film thickness and substrates depending mainly on the metallic precursors and Se adjustment. The surface morphology showed granular structures that increased with the film thickness and TCO substrates.

Acknowledgements This study has been supported by the Spanish Ministry of Science and Innovation through the TEC2007-66506-C02-01/MIC project and CIEMAT Photovoltaic Program.

References

1. Shirakata S, Chichibu S, Matsumoto S, Isomura S (1993) Jpn J Appl Phys 32:L167
2. Repins I, Contreras MA, Egaas B, DeHart C, Scharf J, Perkins CL, To B, Noufi R (2008) Prog Photovoltaics 16:235
3. Marsillac S, Paulson PD, Haimbodi MW, Birkmire RW, Shafarman WN (2002) Appl Phys Lett 81:1350
4. Rockett A, Birkmire RW (1991) J Appl Phys 70:R81
5. Reddy YBK, Raja VS (2006) Mater Chem Phys 100:152
6. Reddy YBK, Raja VS (2002) In: Conference record of the 29th IEEE photovoltaic specialists conference, New Orleans, p 664
7. Marsillac S, Benchouk K, ElMoctar C, Bernede JC, Pouzet J, Khellil AJamali M, Khellil A, Jamali M (1997) J Phys III 7:2165
8. Bernede JC, Marsillac S, Moctar El, Conan A (1997) Phys Stat Sol a Appl Res 161:185
9. López-García J, Guillen C (2009) Thin Solid Films 517:2240
10. Choi IH, Yu PY (2009) Current Appl Phys 9:151
11. Nakada T, Hirabayashi Y, Tokado T, Ohmori D, Mise T (2004) Sol Energy 77:739
12. Nakada T (2005) Thin Solid Films 480:419–425
13. Tokado TNakada T (2003) In: Proceedings of 3rd world conference on photovoltaic energy conversion, Osaka, vols a-C 539
14. Nishiwaki S, Siebentritt S, Walk P, Lux-Steiner MC (2003) Prog Photovolt 11:243–248
15. Young DL, Abushama J, Noufi R, Li XN, Keane J, Gessert TA, Ward JS, Contreras M, Symko-Davies M, Coutts TJ (2002) In: Conference record of the 29th IEEE photovoltaic specialists conference, New Orleans, p 608
16. Guillén C, Herrero J (2008) Vacuum 82:668
17. Guillén C, Herrero J (2006) Thin Solid Films 510:260
18. Caballero R, Guillen C (2005) Sol. Energy Mater Sol Cells 86:1
19. Jost S, Hergert F, Hock R, Purwins M, Enderle R (2006) Phys Stat Sol a Appl Mater Sci 203:2581
20. López-García J, Guillen C (2009) Phys Stat Sol a Appl Mater Sci 206:84
21. El-Boragy M, Szepan R, Schubert K (1972) J Less Common Met 29:133
22. Nozaki HS, Shibata K, Onoda M, Yukino K, Ishii M (1994) Mater. Res. Bull. 29:203–206
23. Bradley AJ, Nature 168: 661
24. Chichibu S, Shishikura M, Ino J, Matsumoto S (1991) J. Appl. Phys. 70:1648–1651
25. López-García J, Guillén, C. (2008) Proc 23rd European Photovoltaic Solar Energy Conference Valencia, Spain

26. West AR (1984) Solid state chemistry and its applications. Wiley, New York
27. Reddy YBK, Raja VS, Sreedhar B (2006) J Phys D Appl Phys 39:5124
28. Marsillac S, Wahiba TB, El Moctar C, Bernede JC, Khelil A (2002) Sol Energy Mater Sol Cells 71:425
29. Joseph CM, Menon CS (1997) Sol State Phenomena 55:226
30. Halgand E, Bernède JC, Marsillac S, Kessler J (2005) Thin Solid Films 480–481:443
31. Green MA (1982) Solar cells-operating principles technology and system applications. Prentice-hall, Englewood Cliffs
32. Bernede JC, Marsillac S, ElMoctar CO, Chouk KB, Khelil A (2001) J Mater Sci 36:87. doi:10.1023/A:1004894825543
33. El Moctar CO, Kambas K, Marsillac S, Anagnostopoulos A, Bernede JC, Benchouck K (2000) Thin Solid Films 371:195
34. Korzoun BV, Makovetskaya LA, Savchuk VA, Rubtsov VA, Popelnyuk GP, Chernyakova AP (1995) J Electron Mater 24:903
35. López-García J, Maffiotte C, Guillén C (2010) Sol. Energy Mater Sol Cells 94:1263